SAND2019-14650C

Molecular-Level Simulation of Compressible Turbulence

M. A. Gallis[1], N. P. Bitter[2], and J. R. Torczynski[3]

Engineering Sciences Center, Sandia National Laboratories, Albuquerque NM 87185, USA

The Direct Simulation Monte Carlo (DSMC) method of molecular gas dynamics (MGD) has been used for more than 50 years to simulate rarefied gas flows. Modern supercomputers have brought higher-density near-continuum flows within range. In the present paper, DSMC is used to study compressible turbulence in the Taylor-Green (TG) vortex flow. The DSMC results are compared to available numerical results from Direct Numerical Simulation (DNS) of the (continuum) Navier-Stokes equations.

I. Introduction

The turbulent energy cascade indicates that, in a statistical sense, kinetic energy is generated at large scales, transferred to progressively smaller scales, and ultimately dissipated by viscosity at the Kolmogorov length scale. This inter-scale transfer of kinetic energy is even more complicated and less well understood for compressible turbulence than for incompressible turbulence. In compressible turbulence, nonlinear interactions of vortices, acoustic waves, shock waves, and expansion waves lead to strong coupling between the velocity field and the thermodynamic fields.

When a compressible fluid is in turbulent motion, its thermodynamic properties (i.e., density, pressure, temperature, specific entropy) and its thermophysical properties (i.e., viscosity, specific heat, thermal conductivity) undergo fluctuations. Measures of these fluctuations need to be included in the specification of the turbulent state. Kovasznay [1] decomposed turbulent fluctuations into three disturbance modes: acoustic, vortical, and entropic. However, this decomposition is defined only for weak fluctuations and spatially uniform thermodynamic properties. In this situation, the three modes are dynamically decoupled from each other to first order in the fluctuation amplitude. However, in compressible flow, mode couplings arise, and any two modes can combine to generate new modes.

The baroclinic interaction between shock waves and vortices creates new vortices, which are amplified by compressibility when density differences and fluctuations are not negligible, thereby increasing the net vorticity. The properties of this compressible turbulence may differ from those of incompressible turbulence: physical phenomena such as thermal fluctuations and translational nonequilibrium may affect baroclinic generation of turbulence. These physical phenomena involve molecular-level processes at the mean-free-path scale and thus are not typically included in Direct Numerical Simulation (DNS) of the Navier-Stokes equations. In contradistinction, these phenomena are inherently captured by molecular-level gas-kinetic methods. Furthermore, all shock-capturing methods degrade to first order in the vicinity of shocks because of the monotonicity requirements. This is particularly important in the initial stage of Taylor Green flow, where shocks first interact with vortices and generate smaller scales in the velocity field.

In this paper, Bird's Direct Simulation Monte Carlo (DSMC) method [2] of molecular gas dynamics (MGD) is used to study compressible turbulence in the Taylor-Green (TG) vortex flow. The remainder of this paper is organized as follows. First, the incompressible TG vortex flow is briefly discussed. Second, the DSMC and DNS methods are briefly reviewed. Third, DSMC and corresponding DNS results for the compressible TG vortex flow examined here are presented, reviewed and compared. Finally, some observations are drawn based on this comparison.

---

[1] Distinguished Member of Technical Staff, Engineering Sciences Center.
[2] Senior Member of Technical Staff, Engineering Sciences Center.
[3] Distinguished Member of Technical Staff, Engineering Sciences Center.

II. Taylor-Green (TG) Flow

Incompressible Taylor-Green (TG) vortex flow [3,4] is a canonical turbulent flow in which the generation of eddies and the corresponding cascade of energy from small to large wavenumbers can be observed numerically. TG flow is initialized in a triply periodic domain $-\pi L \le \{x,y,z\} \le \pi L$ using velocity and pressure fields having only a single length scale L and a single velocity scale V_0:

$$\begin{aligned} u &= V_0 \sin(x/L)\cos(y/L)\cos(z/L) \\ v &= -V_0 \cos(x/L)\sin(y/L)\cos(z/L) \\ w &= 0 \\ p &= p_0 + (\rho_0 V_0^2/16)(\cos(2x/L)+\cos(2y/L))(\cos(2z/L)+2) \end{aligned} \quad . \tag{1}$$

Here, $\mathbf{u} = (u,v,w)$ is the velocity and p is the pressure at position $\mathbf{x} = (x,y,z)$ and time $T = 0$, where $T = V_0 t/L$. Thus, all of the kinetic energy is initially resident in a single wavenumber. The initial density is set by assuming a spatially uniform initial temperature of 273.15 K.

The DSMC code SPARTA [5,6] is used to simulate TG flow. The domain length scale is $L = 0.0001$ m. The domain is subdivided into 8 billion cells (2000^3) with an average of 45 particles per cell for a total of 0.36 trillion particles. The time step is 3 ps. The gas has molecular mass $m = 66.3\times10^{-27}$ kg specific heat ratio $\gamma = 5/3$, and reference-property values at STP (101325 Pa, 273.15 K) for pressure, temperature, and density. The (maximum) velocity V_0 corresponds to a Mach number of 0.3, 0.6, 0.9, and 1.2 and Reynolds number of 500, 1000, 1500, 2000. For the Mach 0.3 case, the long-time temperature increase is roughly 1%. These conditions marginally satisfy the incompressibility assumption, while for all the other ones, compressibility effects are increasingly present.

III. DSMC Method

The DSMC method [2] uses computational molecules, or "particles", to represent a gas flow. Each particle represents a large number of real molecules, and these particles move, reflect from solid boundaries, and collide with each other so as to reproduce the statistical behavior of real molecules. The computational domain is divided into rectangular cells for two-dimensional or axisymmetric simulations and into cuboidal cells for three-dimensional simulations. Objects are represented as triangulated surfaces that intersect these cells. During each time step, molecules move ballistically at constant velocity over the time step, which may involve reflections from solid surfaces, and then collide stochastically in a pairwise fashion with other particles in the same cell. Particles reflect from solid boundaries specularly, diffusely at the boundary temperature, a combination of these processes, or by more complex processes. Particle-particle collisions are performed using hard-sphere (HS), variable-hard-sphere (VHS), or variable-soft-sphere (VSS) interactions [2]. Sampling the properties of the particles within each cell yields flow properties for each cell. Typically, the cell size and the time step are smaller than the mean free path and the mean collision time, respectively.

Like most molecular methods, DSMC simulations are "noisy": the flow quantities associated with a cell fluctuate as particles move into and out of the cell. For example, the flow velocity associated with a cell fluctuates about its mean value with a variation that scales with the gas-molecule thermal speed divided by the square root of the number of particles in the cell.

Essentially incompressible flows present a challenge for DSMC in that the flow speed is much smaller than the gas-molecule thermal speed (a "low-speed" flow). Thus, large numbers of particles per cell would seem to be required to resolve the flow. This difficulty is mitigated by averaging cell-based quantities over multiple time steps and thereby effectively acquiring many more samples per cell, which reduces noise to an acceptable level. The temporal averaging duration is chosen to be much smaller than the smallest macroscopic (hydrodynamic) time scale.

Hydrodynamic flows present another challenge for DSMC in that the mean free path is small relative to the domain (a "high-density" flow). Since the cells are small relative to the mean free path, a large number of cells is required for such a simulation. This large number of cells necessitates using modest numbers of particles per cell (e.g., 10-100), which in turn motivates the use of the temporal averaging discussed above.

Thus, a DSMC simulation of an essentially incompressible flow requires an extremely large computational effort to resolve all length scales from molecular to hydrodynamic while achieving an acceptable signal-to-noise ratio. The required computational effort has generally prevented DSMC (and other molecular-level methods) from being used to simulate flows in the hydrodynamic (continuum) regime. Three recent exceptions are simulations of the Richtmyer-Meshkov and Rayleigh-Taylor instabilities and the incompressible Taylor-Green vortex by Gallis et al. [7,8,9].

All DSMC simulations presented herein are performed with SPARTA, an open-source DSMC code developed and maintained by Sandia National Laboratories [5,6]. SPARTA is an exascale-class open-source code capable of running efficiently on massively parallel, heterogeneous-architecture computational platforms.

Molecular collisions are performed using the VSS model [2]. To improve the spatial discretization, collision partners are selected from within a sphere having a radius that equals the distance traveled by the particle during a time step [10]. Multiple collisions between the same molecules during the same time step are not allowed, in accord with molecular chaos for collisions.

IV. DNS Solver

The DSMC results are compared to Direct Numerical Simulations (DNS) executed using the code US3D, developed at the University of Minnesota [11]. This code is a shock-capturing finite volume code which is capable of achieving both stability in the presence of strong shock waves and reasonably high accuracy in smooth regions of the flow. This is accomplished by blending two numerical methods. The first is the modified Steger-Warming method [12], which offers good numerical stability but generates significant numerical dissipation. The second is the kinetic energy consistent scheme of Subbareddy and Candler [13], a central-difference scheme which delivers sixth-order spatial accuracy and lower numerical dissipation at the expense of reduced numerical stability. Using this approach, the code switches between these two schemes using gradients in the Mach number to detect shocks and apply the stabilizing modified Steger-Warming fluxes in those regions. The result is an overall scheme with good accuracy in smooth parts of the flow that is robust to shock waves. For simulations at the highest Mach number (Mach 1.2), this blended scheme is used. For simulations at lower Mach numbers (Mach 0.3, 0.6, 0.9), only the more accurate kinetic energy consistent scheme is used since any shocklets produced are not strong enough to destabilize the method. Time advancement is accomplished using a third-order explicit Runge-Kutta method with a Courant-Friedrichs-Lewy number of 0.5 to determine the time step.

The fluid is modeled as a monatomic gas (argon) with a power-law viscosity model having an exponent of 0.66 and a Prandtl number of 0.669. For initial conditions, the velocity and pressure fields are set using the classic, incompressible Taylor Green vortex, given in Equation (1), and the density is set by assuming a constant initial temperature of $T_o = 273.15K$. The Mach number of the vortex is set by the characteristic velocity, and the Reynolds number is set by adjusting the viscosity at the reference temperature T_o .

The simulation domain is a cube having sides of length $2\pi L$ with periodic boundary conditions. The domain is discretized using 600 points along each edge. To check for grid convergence, the simulations were also run with 400 points along each edge, and the dissipation versus time was found to be indistinguishable for Mach 0.3-0.9. For Mach 1.2, some differences between the 400^3 and 600^3 meshes were observed, so additional simulations were run using the Sandia Parallel Aerodynamics and Reentry Code (SPARC) [14,15], employing the same numerical method described above. Using SPARC made it possible to perform simulations with grids having as many as 1024 points on each edge of the domain. The volume-averaged viscous dissipation rate from the SPARC simulations on the 1024^3 grid was found to differ by less than 3% from the US3D simulations on a 600^3 grid over the time interval $0 \le T \le 20$, indicating that the results are sufficiently grid converged. To further check the adequacy of the numerical scheme that was used, SPARC was also run using a Weighted Essentially Non-Oscillatory (WENO) finite difference scheme [15] and the results were found to agree with the blended method described above.

V. Results and Discussion

Figure 1 presents the DSMC and DNS energy dissipation rates as functions of time. The DSMC and DNS results are in good qualitative agreement for all Mach numbers and over the entire time period during which the energy dissipation rate is significant, although some differences appear at the time of maximum dissipation. For all Mach numbers, both methods yield the same rapid increase from $T = 2$ to $T = 6$, the same plateau from $T = 6$ to $T = 10$, the same maximum between $T = 8$ and $T = 9$, the same rapid decrease from $T = 9$ to $T = 15$, and the same slow decrease from $T = 15$ to $T = 20$. DSMC does generally yield a slightly faster energy dissipation rate than DNS although, in the Ma = 1.2 case, there are instances where the DSMC dissipation rate falls below the DNS dissipation rate. Differences in the dissipation rate appear for the Ma = 0.3-0.9 cases around the time of maximum dissipation and for the Ma = 1.2 case from $T = 6$ onward.

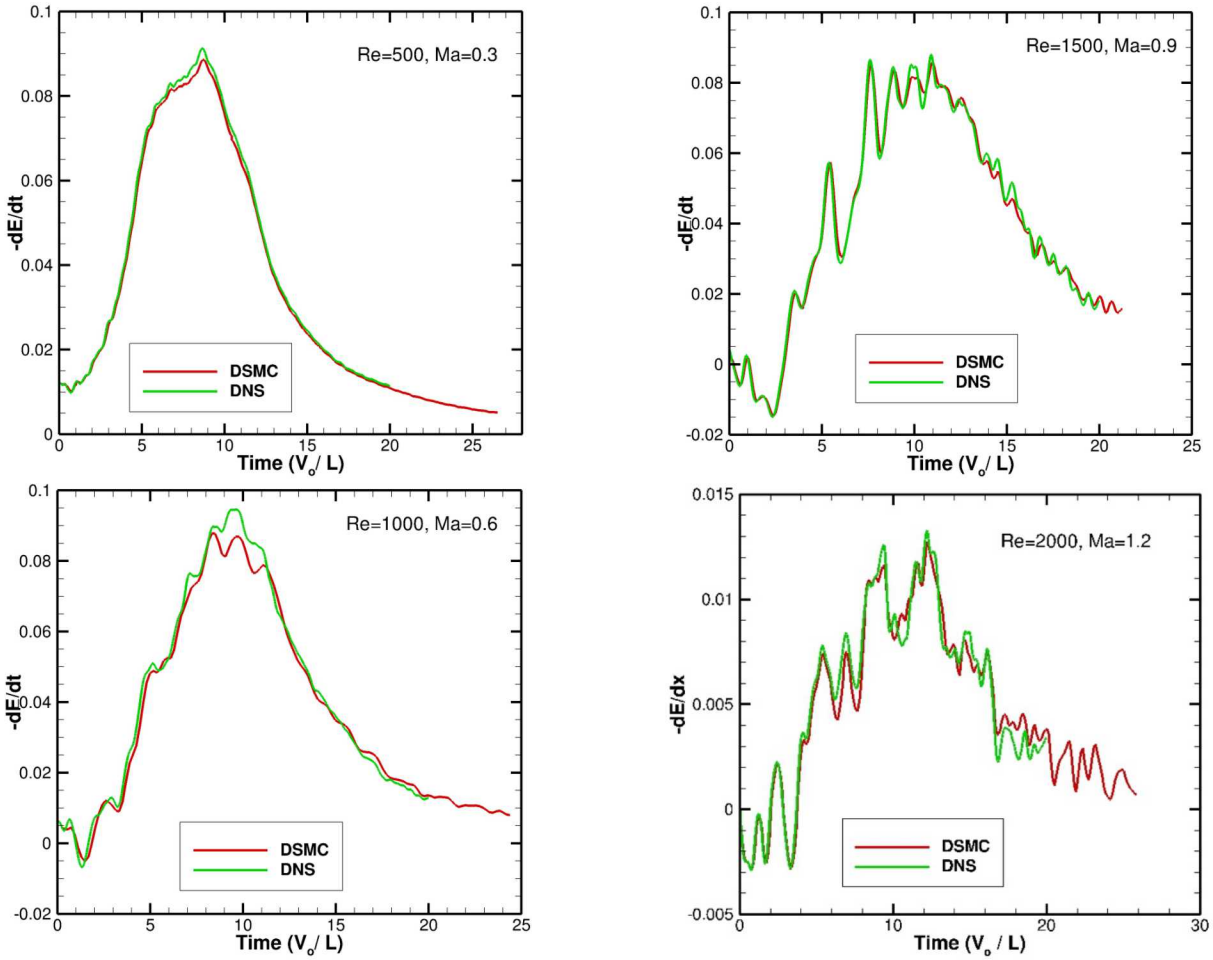

Fig. 1. Energy dissipation rate as a function of time for several Mach numbers.

Figures 2-9 present the u velocity component on the bounding planes of the domain from the DSMC simulations (left) and the DNS simulations (right). There are two sets of figures for each case: one near the maximum dissipation point and a second one at a point during the decay of turbulence well past the maximum dissipation time. Below each three-dimensional picture, the top (y-z) plane is plotted separately to allow easier comparison of this plane.

Except for being slightly noisy, the DSMC molecular results are virtually identical to the DNS Navier-Stokes results for the point of maximum dissipation at all Mach numbers. At that time, the large-scale structures that are the remnants of the initial conditions are clearly discernible, but smaller-scale structures are also present.

The DSMC and DNS flow fields for Mach numbers greater than 0.6 and at times past the maximum dissipation time, however, exhibit visible differences, especially on the y-z plane. The DSMC simulations have richer structures with finer features than the DNS simulations have. In the y-z plane, in particular, the late-time DSMC fields exhibit significant velocity fluctuations that are 10 times larger than fluctuations observed in the DNS simulations.

It is well established that shock waves can generate new turbulence [16]. When the turbulent Mach number is of order unity, the turbulence properties differ substantially from the incompressible situation because physical phenomena at the mean-free-path level, such as thermal fluctuations and translational non-equilibrium, may play a role in the baroclinic creation of turbulence. These phenomena are typically not included in the Navier-Stokes equation but, in contradistinction, are inherently captured by molecular-level kinetic simulations. The appearance of these fluctuations at later times for Mach numbers above 0.3, along with the simultaneous appearance of finer structures on the other planes, could be attributed to baroclinic creation of vorticity between shocklets, which appear in the high-Mach-number cases, and thermal fluctuations. In this case, a new mode of turbulent fluctuations needs to be added to the Kovasznay analysis, namely turbulent fluctuations caused by the interaction of thermal fluctuations and shocks or shocklets in the flow field.

Since DSMC assumes a statistical description of the gas, each particle in the DSMC simulation represents approximately 10,000 real molecules (the "simulation ratio"), so it is reasonable to question whether these fluctuations are a numerical artifact of the DSMC simulations. To investigate this assertion, simulations with half and double simulation ratios were performed. It is reassuring to observe that changes to the simulation ratio did not affect the amplitude of these fluctuations. This suggests that these fluctuations are not numerical artifacts but are hydrodynamic features of the DSMC simulations.

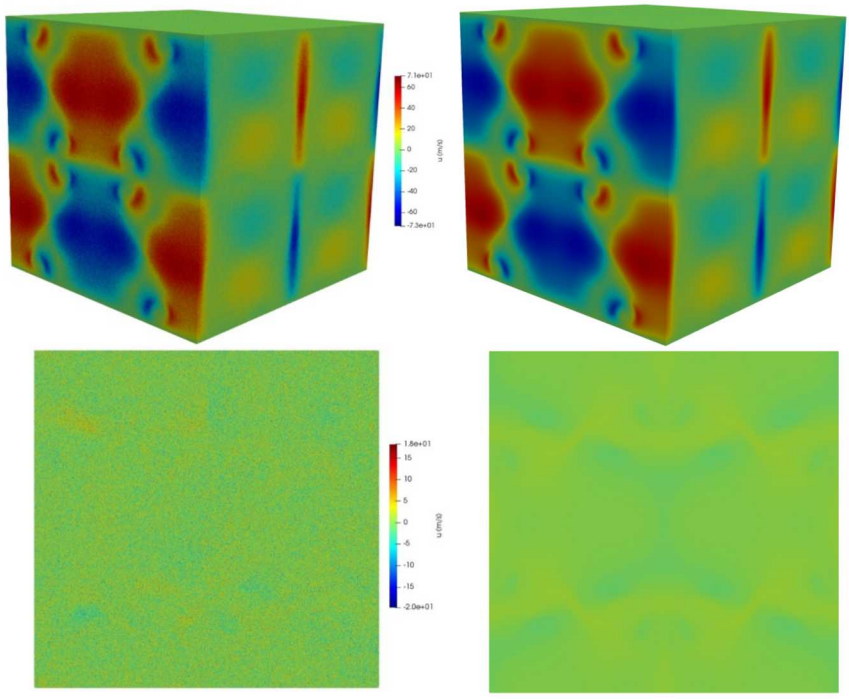

Fig. 2. DSMC (left) and DNS (right) u velocity fields for Ma = 0.3 at $T = 8.7$.

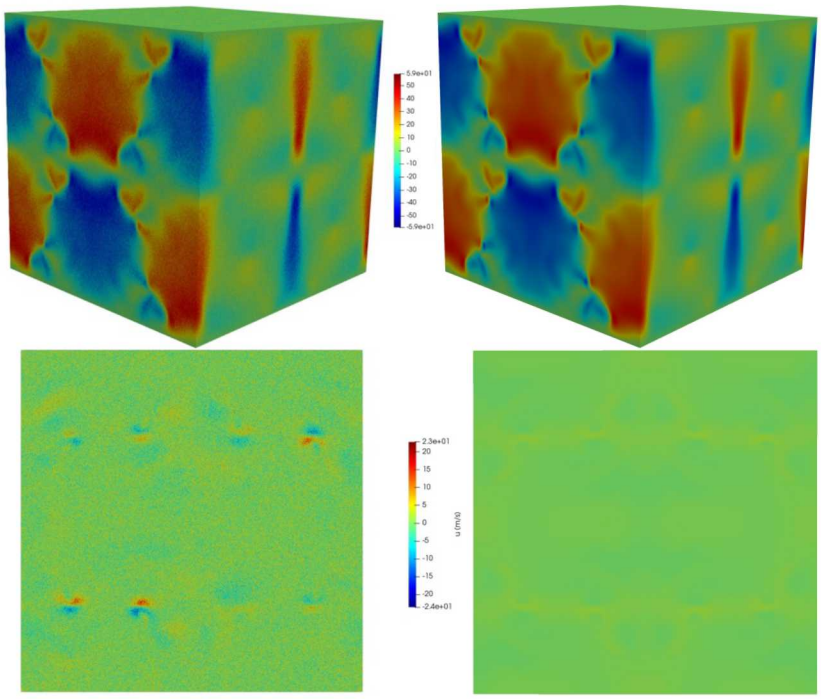

Fig. 3. DSMC (left) and DNS (right) u velocity fields for Ma = 0.3 at $T = 12.1$.

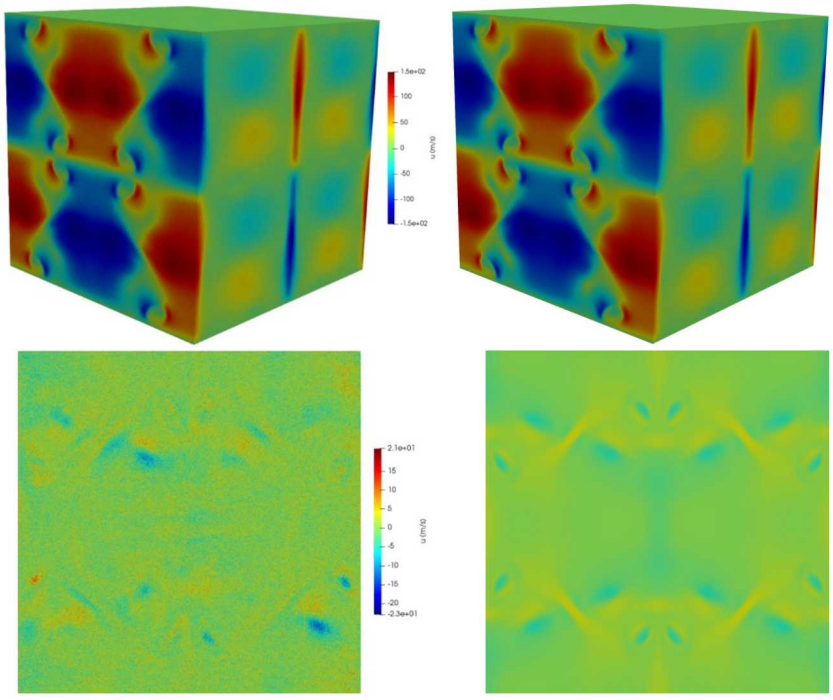

Fig. 4. DSMC (left) and DNS (right) u velocity fields for Ma = 0.6 at $T = 8.45$.

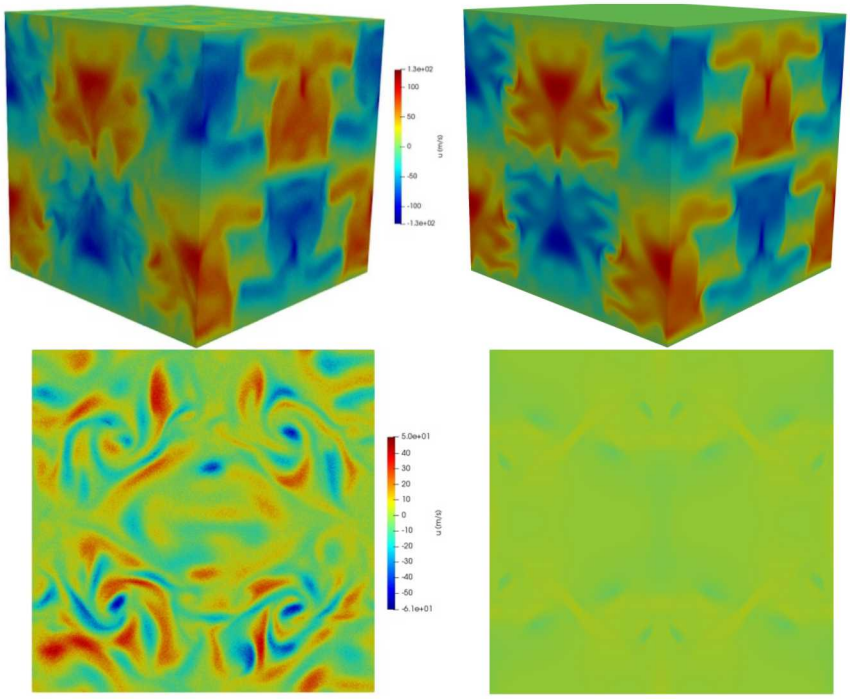

Fig. 5. DSMC (left) and DNS (right) u velocity fields for Ma = 0.6 at $T = 18.47$.

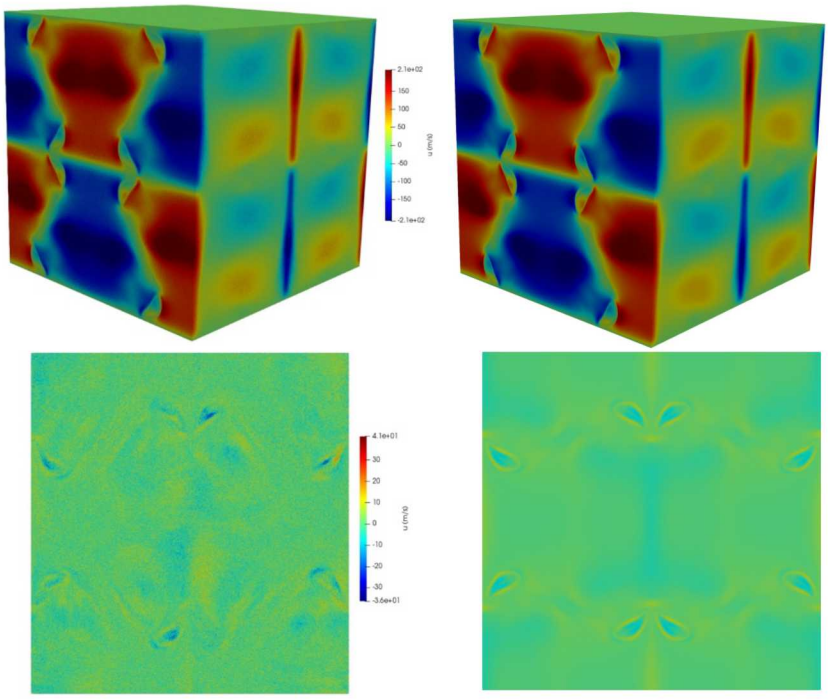

Fig. 6. DSMC (left) and DNS (right) u velocity fields for Ma = 0.9 at $T = 7.63$.

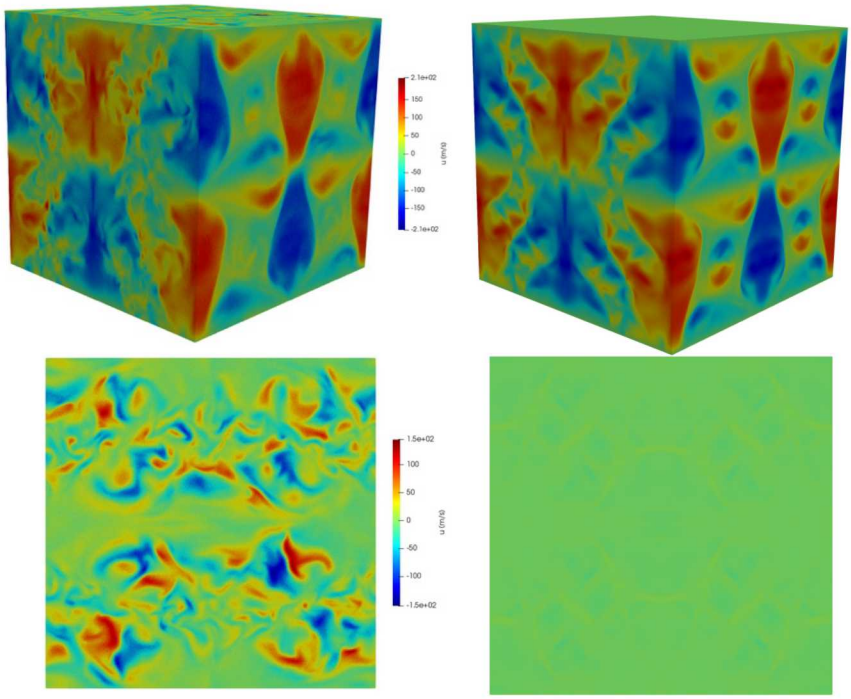

Fig. 7. DSMC (left) and DNS (right) u velocity fields for Ma = 0.9 at $T = 14.77$.

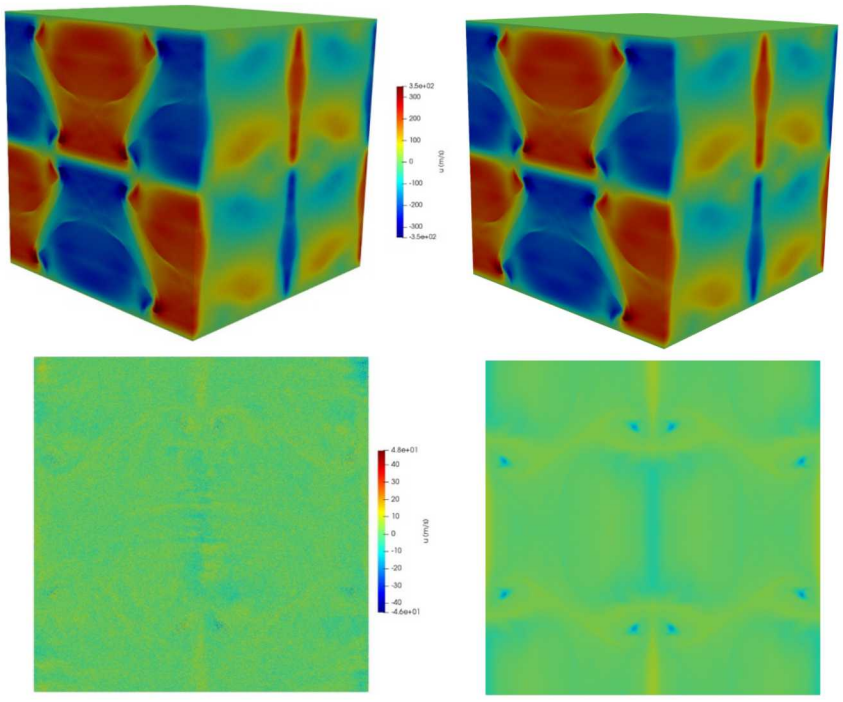

Fig. 8. DSMC (left) and DNS (right) u velocity fields for Ma = 1.2 at $T = 6.87$.

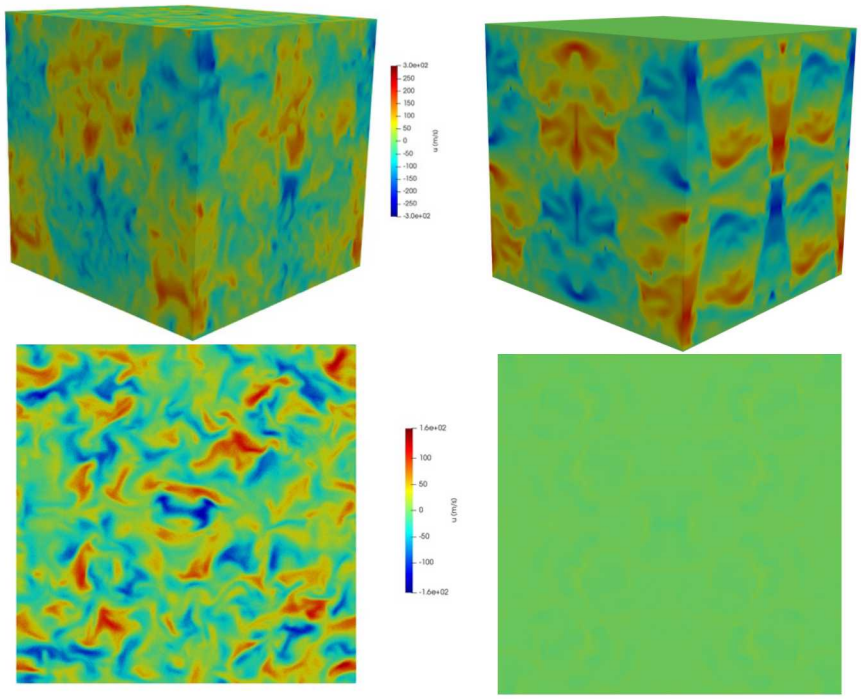

Fig. 9. DSMC (left) and DNS (right) u velocity fields for Ma = 1.2 at T = 18.56.

VI. Conclusions

Several compressible Taylor-Green (TG) vortex-flow simulations were performed using the DSMC method. Results for the energy dissipation and u-velocity fields were compared to Direct Numerical Simulation (DNS) results for the (continuum) Navier-Stokes equations. It is observed that the two techniques are in good agreement for low Mach numbers (0.3 and 0.6). As the Mach number increases, differences appear in both dissipation rates and velocity profiles, especially beyond the point in time at which the maximum dissipation occurs. In all cases at late times, the DSMC simulations exhibit flow structures that are not seen in the DNS simulations, especially on the y-z plane. These differences could be attributed to baroclinic creation of vorticity due to the interaction of shocklets and thermal fluctuations, the latter of which are present only in the DSMC simulations.

Acknowledgments

Sandia National Laboratories is a multimission laboratory managed and operated by National Technology and Engineering Solutions of Sandia, LLC, a wholly owned subsidiary of Honeywell International, Inc., for the U.S. Department of Energy's National Nuclear Security Administration under contract DE-NA0003525.

This paper describes objective technical results and analysis. Any subjective views or opinions that might be expressed in the paper do not necessarily represent the views of the U.S. Department of Energy or the United States Government.

This manuscript has been authored by National Technology and Engineering Solutions of Sandia, LLC, under Contract No. DE-NA0003525 with the U.S. Department of Energy. The United States Government retains and the publisher, by accepting the article for publication, acknowledges that the United States Government retains a non-exclusive, paid-up, irrevocable, world-wide license to publish or reproduce the published form of this manuscript, or allow others to do so, for United States Government purposes.

References

1. Kovasznay, L. S., "Turbulence in Supersonic Flow," *Journal of the Aeronautical Sciences,* **20** (10), 657-682, 1953.
2. Bird, G. A., *Molecular Gas Dynamics and the Direct Simulation of Gas Flows*, Clarendon Press, Oxford, 1998.
3. Taylor, G. I., and Green, A. E., "Mechanism of the Production of Small Eddies from Large Ones," *Proceedings of the Royal Society of London, Series A,* **158** (895), 499-521, 1937.
4. Brachet, M. E., Meiron, D. I., Orszag, S. A., Nickel, B. G., Morf, R. H., and Frisch, U., "Small-scale structure of the Taylor-Green vortex," *Journal of Fluid Mechanics,* **130**, 411-452, 1983.
5. Plimpton, S. J., and Gallis, M. A., "SPARTA Direct Simulation Monte Carlo (DSMC) Simulator," http://sparta.sandia.gov, 2015.
6. Plimpton, S. J., Moore, S. G., Borne, A., Stagg, A. K., Koehler, T. P., Torczynski, J. R., and Gallis, M. A., "DSMC on petascale machines and beyond," *Physics of Fluids*, **31** (8), 086101, 2019.
7. Gallis, M. A., Koehler, T. P., Torczynski, J. R., and Plimpton, S. J., "Direct simulation Monte Carlo investigation of the Richtmyer-Meshkov instability," *Physics of Fluids,* **27** (8), 084105, 2015.
8. Gallis, M. A., Koehler, T. P., Torczynski, J. R., and Plimpton, S. J. "Direct simulation Monte Carlo investigation of the Rayleigh-Taylor instability," *Physical Review Fluids,* **1**, 043403, 2016.
9. Gallis, M. A., Koehler, T. P., Torczynski, J. R., Plimpton, S. J., and Papadakis, G., "Molecular-Level Simulations of Turbulence and Its Decay," *Physical Review Letters,* **118**, 064501, 2017.
10. Bird, G. A., Gallis, M. A., Torczynski, J. R., and Rader, D. J., "Accuracy and efficiency of the sophisticated direct simulation Monte Carlo algorithm for simulating noncontinuum gas flows," *Physics of Fluids* 21 (1), 017103, 2009.
11. Candler, G. V., Johnson, H. B., Nompelis, I., Subbareddy, P. K., Drayna, T. W., Gidzak, V., and Barnhardt, M. D., "Development of the US3D Code for Advanced Compressible and Reacting Flow Simulations," AIAA Paper 2015-1893, 2015.
12. MacCormack, R. W., and Candler, G. V., "The Solution of the Navier-Stokes Equations using Gauss-Seidel Line Relaxation," *Computers & Fluids*, **17** (1), 135-150, 1989.
13. Subbareddy, P. K., and Candler, G. V., "A Fully Discrete, Kinetic Energy Consistent Finite-Volume Scheme for Compressible Flows," *Journal of Computational Physics*, **228** (5), 1347-1364, 2009.
14. Howard, M., Bradley, A. M., Bova, S. W., Overfelt, J. R., Wagnild, R. M., Dinzl, D. J., Hoemmen, M. F., and Klinvex, A., "Towards a Performance Portable Compressible CFD Code," AIAA Paper 2017-4407, 2017.
15. Maeng, J. B., Fisher, T. C., and Carpenter, M. H., "Generalized Entropy Stable Weighted Essentially Non-Oscillatory Finite Difference Schemes in Multi-Block Domains," AIAA Paper 2019-3205, 2019.
16. Grinstein, F. F., *Coarse Grained Simulation and Turbulent Mixing*, Cambridge University Press, 2016.